Effects of Hydrocarbon Fuel Structure on Experimental Laminar & Turbulent Burn Rates

A.A. Burluka[1], R.G. Gaughan[2], J.F. Griffiths[3], C. Mandilas[*,1], C.G.W. Sheppard[1], R. Woolley[4]

[1] School of Mechanical Engineering, The University of Leeds, Leeds LS2 9JT, UK
[2] ExxonMobil Research and Engineering Company, Paulsboro Technical Center, Paulsboro, NJ 08066, U.S.A
[3] School of Chemistry, University of Leeds, Leeds, LS2 9JT, UK
[4] The University of Sheffield, Department of Mechanical Engineering, Mappin Street, S1 3JD, UK
[*] Corresponding Author's Current Address, Aerosol and Particle Technology Laboratory, Thermi, 57001, Greece

Abstract

Experimental measurements of laminar and turbulent burn rates have been made for premixed fuel-air flames of hydrocarbons (HC) with six carbon atoms including unsaturated, cyclic and branched molecules. Measurements were performed at 0.5 MPa, 360 K and turbulent rms velocities of 2 and 6 m/s for a range of equivalence ratios. The laminar burning velocities were used to interpret the turbulent data. The measured laminar burning velocities showed dependence on the molecular structure. The burn rate ranking of fuels observed in the laminar measurements was to a degree retained in the turbulent experiments. The equivalence ratio of peak turbulent burn rates was different to that under laminar conditions and was found to be a function of the rms turbulent velocity (u').

Introduction

Burning velocity has been the subject of numerous experimental and theoretical investigations spanning many decades as it affects engine performance, efficiency and cycle-to-cycle variability. Understanding the factors that influence the burn rate enables better control of engine combustion quality and emissions. The combustion rate in an engine is a function of the turbulent burning rate, which is itself a function of those physico-chemical features of a fuel-air mixture encapsulated in its laminar burning velocity and the turbulence characteristics of the flow field within the engine. The influence of fuel structure on the laminar burning velocity is well studied [e.g. 1-5]. However, published data on the influence of HC molecular structure on burn rate under turbulent conditions is very sparse and recent [6]. The primary aim of the current work was to investigate fuel structure and equivalence ratio effects on the laminar and turbulent burning rates of deflagrations in a spherical combustion vessel.

Presented in this paper are experimentally determined laminar and turbulent burn rates for a set of HCs of varied structure, but common carbon number, C_6. The fuels examined were 2,2-dimethyl butane, 2-methyl pentane (isohexane), n-hexane, cyclohexane, 1-hexene, cyclohexene and 1-hexyne. With the exception of 1-hexyne, all other fuels are representative components of gasoline blends.

Experimental and Results Processing

The Leeds MkII spherical bomb was employed for the studies. For reasons of brevity, description of the equipment and experimental procedure is omitted here. Nonetheless, the interested reader is referred to published work describing equipment and procedure in detail [7-8]. The results reported here refer to schlieren based measurements. All deflagrations were initiated at initial temperature and pressure of 360 K and 0.5 MPa, where published experimental data are relatively sparse. This relatively high initial temperature ensured complete fuel vapourisation and contributed to the avoidance of condensation on the walls and windows after ignition, while the elevated initial pressure was adopted to provide conditions relevant to combustion in internal combustion engines. In the early stages of combustion, for flames of mean flame radius less than the window diameter, pressure and associated unburned gas temperature remained close to the initial values. Experiments were conducted for $0.78 \leq \phi \leq 1.67$. At least two laminar and five turbulent deflagrations were performed at each condition. Imaging data analysis to determine laminar and turbulent burning characteristics followed established techniques, detailed elsewhere [9-10] and widely used [11-16].

Results and Discussion

Flames for $\phi > 1.1$ for the C6 fuels examined showed signs of hydrodynamic instabilities (cellularity) as early as a mean flame radius of 10-15 mm. Consequently, too few data points were available to determine the Markstein length, L_b and thus fit the data accordingly for determination of the 1D stretch free burn rate, u_l. Laminar burning velocity results for the C_6 group of HC are displayed in Fig. 1. Solid lines refer to results obtained by extrapolating the measured flame speeds to zero stretch then dividing the flame speed by the density ratio [10]. Normal lines refer to data obtained via application of traditional u_l theory [9], while dotted lines correspond to u_l values computed using $u_l = u_{n,min}$, where, u_n is the stretched entrainment burning velocity. Burning velocities obtained in this way cannot be considered to be accurately defined but represent a pragmatic approach to obtaining laminar burning velocity data to aid the analysis of subsequent turbulent burning measurements.

The u_l of the C6 fuels peaked close to $\phi = 1.1$ and demonstrated a dependence on molecular structure that

[*] Corresponding author: mandilas@cperi.certh.gr

was similar at all ϕ. Overlaps in u_l ranking were evident only in the richest mixture setting explored, where the impact of cellularity is greatest. The highly unsaturated fuels 1-hexyne (triple C≡C bond) and cyclohexene (double C=C and ring structure) had the highest u_l. Ranking of the remaining fuels was: 1-hexene (unsaturated, double C=C bond), cyclohexane (unsaturated, ring structure) and n-hexane (saturated). The iso-alkanes burned slowest, with the double branched 2,2 dimethyl butane noticeably slower than the single branched 2-methyl pentane. Analogous observations were made from burning velocities measured in a constant volume combustion vessel at similar initial conditions [4]. For cross-reference, it is noted that the laminar burn rates reported here for n-hexane are very similar (within 5%) to those published in [17], at identical P_i and T_i conditions.

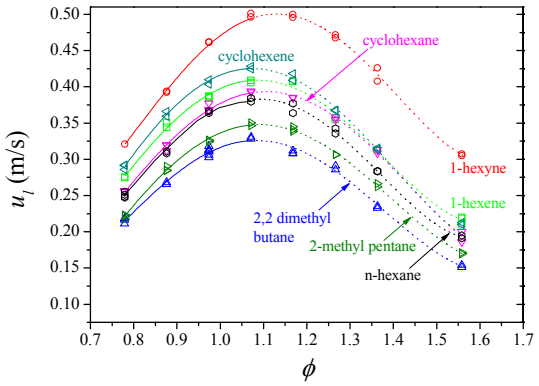

Fig. 1 – Laminar burning velocities vs ϕ for the C_6 fuels.

The diffusive properties of a mixture are characterised by the Lewis number and Markstein length, Le and L_b. The Markstein length of a flame is a physicochemical factor, typically used to characterise the effect of total stretch rate on flame speed [18]. In this work, L_b values were approximated as the slope of the linear fit of the flame speed vs stretch rate curve, as described in [10]. The values of L_b obtained via this method were compared against values obtained with the use of a non-linear method for calculating L_b [19]. The results were found to be similar, arguably because the L_b values at the conditions explored were close to zero.

High positive values of L_b indicate that as the flame expands, and becomes increasingly less stretched, there is a gain in flame speed; the opposite is true for flames with negative L_b values. Although of notable scatter, with COV as high as 25% [8], differences in the L_b values measured for the C_6 fuels (at fixed ϕ) were small. The overall trend revealed a decrease in L_b with equivalence ratio. Nevertheless, L_b values remained positive at all equivalence ratios for which Markstein lengths could be experimentally measured (Fig. 5). This high similarity in the L_b of the various C6 fuels is primarily attributed to their similar thermo-diffusive characteristics, arising from their similar molar mass.

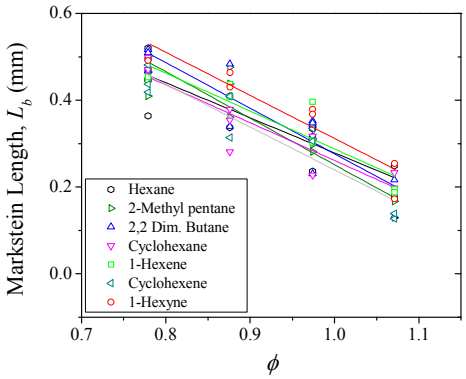

Fig. 2 – Measured Markstein lengths for the C_6 fuels.

Lewis number is defined as the ratio of thermal diffusivity of the mixture over the mass diffusivity of the deficient reactant. In the current work, Le values were determined to be equal to α_{mix} / D_i, where the former is the average thermal diffusivity of the mixture and the latter is a mixture-average mass diffusion coefficient of any species i with respect to the total air-fuel mixture. The calculation to obtain Le followed the approach in [20], which is a modified version of the kinetic theory. Due to their very similar molar mass, the C_6 fuels studied were found to have almost identical Le values at lean conditions, where the deficient reactant is the fuel. At rich conditions, the deficient reactant is air, hence Le was almost identical (Table 1).

Table 1 – Lewis numbers against ϕ, computed at T_i and P_i on the basis of the kinetic theory of ideal gases [20].

ϕ	n-hexane	iso-hexane	2,2 dimethyl butane	cyclo-hexane	1-hexene	cyclo-hexene	1-hexyne
0.80	2.58	2.54	2.50	2.50	2.50	2.48	2.43
0.99	2.51	2.48	2.44	2.45	2.44	2.43	2.37
1.40	0.93	0.93	0.93	0.95	0.93	0.95	0.94

Consequently, and taking into account Lewis number effects on cellularity [21], it was expected that flame front instability effects would also be similar for the C_6 HC tested. For schlieren based measurements, the onset of cellularity has been described via the critical flame radius (r_{crit}), i.e. the point where small scale cells appear on the flame surface [22]. It is implicit that due to the progressively growing nature of flame cells, defining r_{crit} from photographic observations is subjective to the human eye. Nonetheless, for all flames examined, this photographic onset of cellularity was relatively clearly definable. Results are shown in Fig. 3. Owing to the positive and negative Le of all fuels explored at lean and rich conditions, the critical flame radii showed a distinctive trend with values being reduced with equivalence ratio. At $\phi > 1.3$, all flames had become fully cellular prior to reaching 10 mm in r_u.

The large thermo-diffusive similarities of the C_6 fuels are further illustrated via the sample flame acceleration (α_f) results of Fig. ?, with very similar trends between the fuels. It is known that the prominent effect of cellularity is to accelerate the burn rate [22]. At the extreme lean condition tested and within the vicinity of the vessel windows all flames had a mean

acceleration of ~0.5 m/s^2. Since there were no signs of flame instability in that region, this low α_f could be due to stretch rate effect artefacts in the burning velocity data or due to slight increase in the P and T inside the vessel. For rich mixtures it was found that the critical flame radii values correlated well with the onset of apparent flame acceleration. Interestingly, the onset of cellularity was followed by a sudden increase in acceleration. Flame acceleration peaked ~10-15 mm in mean flame radius after r_{crit}, before being reduced back to values similar to those observed during the pre-cellular region. It could thus be speculated that flame acceleration is caused due to the transition from a smooth surfaced flame into a fully cellular flame and the subsequent increase in flame surface area, A_f. Once a constant, fully developed cell size is reached, the cellularity induced increase in A_f per unit volume of the flame and consequent acceleration, ceases.

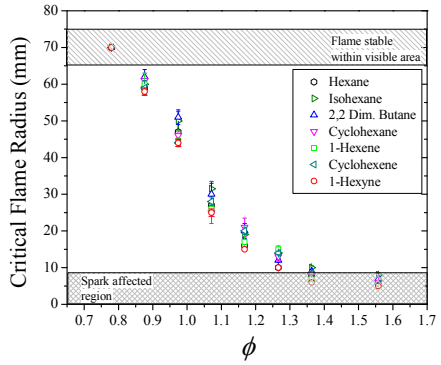

Fig. 3 – Apparent onset of cellularity based on photographic observations.

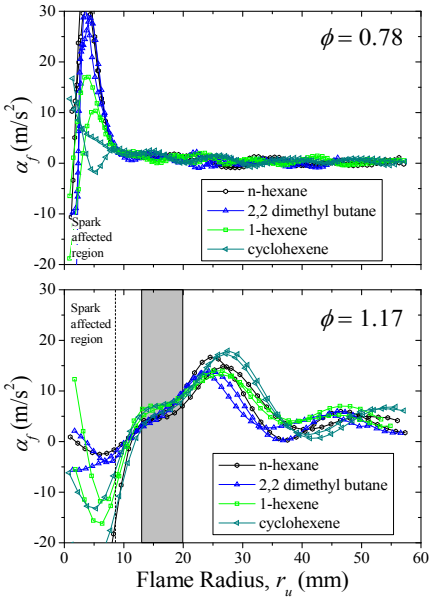

Fig. 4 – Laminar flame acceleration results, including the flame radii (r_{crit}) region where flames became fully cellular (gray-shaded area). Trends shown here were typical of all conditions explored (fuel and ϕ).

The magnitude of u_l has been linked to the adiabatic flame temperature, T_{ad} [2]. Being a function of the enthalpies of the reactants and products, T_{ad} is dependent on the molecular structure and the nature of the chemical bonds of the fuel molecule. Higher flame temperatures both accelerate reaction rates and increase mass and heat transport rates of species at the flame front, thus enhancing u_l. Computations of the T_{ad} suggested an overall correlation with u_l, with overall ranking with respect to u_l being identical to that observed for T_{ad} at all ϕ studied [8]. Nonetheless, relative differences in the T_{ad} between the various fuels investigated were at all conditions lower by as much as an order of magnitude c.f. those in u_l. Similar findings have been reported elsewhere [5]. It is thus implicit that T_{ad} cannot solely explain differences in u_l between fuels, and kinetic differences are also of high importance. Using the suggestions in [4-5, 23-25], kinetics related reasons for the differences in u_l are given below.

Unsaturated HCs have higher burn rates than saturated ones. A lower proportion of H atoms available in the "radical pool" formed during oxidation leads to a weaker propensity for chain branching reactions to boost burn rate. Hydrogen atoms are more easily abstracted from unsaturated molecules (i.e. 1-hexyne, 1-hexene, cyclohexene) due to the presence of the relatively weaker allylic C-H bond. This promotes an additional kinetic advantage to the effect of their higher T_{ad}. There is also a larger number of combustion routes for the break-down of alkenes and alkynes via ethyl radicals, producing extremely fast burning intermediate species, such as ethylene, vinyl radical and acetylene.

Branched alkanes combust slower than their straight chain equivalent. Combustion of the branched alkanes (i.e. 2,2 dimethyl butane and 2-methyl pentane) produces more relatively non-reactive CH3 radicals, compared to n-hexane oxidation, which contributes to a reduction in the overall burn rate. The lower u_l of the branched alkanes can also be related to the propensity of H abstraction during oxidation. For example, in the case of 2,2 dimethyl butane, four out of the six carbon atoms constitute methyl radicals with strong C-H bonds (ΔH^o ~430 kJ/mol); with only two methylene groups, possessing weaker C-H bonds (ΔH^o ~405 kJ/mol). However, 2-methyl pentane contains only three methyl groups and, consequently, 3 methylene groups and consequently has a slightly higher burning velocity than 2,2 dimethyl butane.

Moving onto the turbulent flame results, exemplar experimental values of turbulent burning velocity against flame radius are shown in Fig. 17 for n-hexane at close to stoichiometric conditions. The trend of turbulent flame development of Fig. ?? was similar for all flames studied. Turbulent flames growing in a closed volume accelerate [4, 7, 8, 26] and in order to achieve a consistent comparison it is necessary to define the burning velocity and an appropriate reference point. For this cause, a turbulent burning velocity based on an entrainment of unburned gas, u_{te}, has been adopted [27]. A mean flame radius, r_{sch}, was determined from 2D projected flame area of the schlieren images assuming spherical shape, and the turbulent flame speed was

given by $S_{te} = d_{rsch} / dt$. The burning velocity was then determined by accounting for the expansion of the burned gas, $u_{te} = (\rho_b / \rho_u).S_{te}$.

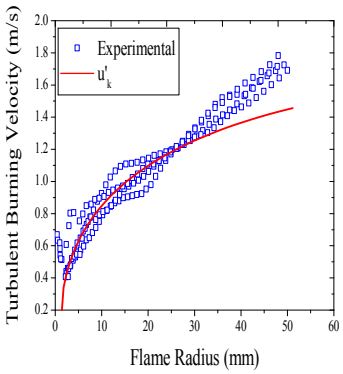

Fig. 5 – Exemplar turbulent flame growth at u' = 2 m/s for n-hexane-air mixtures at $\phi = 0.98$.

This definition of turbulent burning velocity derived from schlieren measurements has been compared with other definitions obtained using pressure transducers and laser sheet measurements [28-29]. The burning velocity was compared at a flame radius, r_{sch} = 30mm. The comparison of turbulent burning velocities at a fixed size may result in uncertainties as the selected radius was not attained at the same dimensionless time, e.g. time from ignition / integral time scale. Since turbulent properties (u' and integral length scale, L) are fixed, comparison differences in time taken for flames to propagate across the vessel arise from different u_l and in particular ρ_b / ρ_u. At a flame radius of r_{sch} = 30 mm, residual consequences of the initiation spark energy were excluded [10]. Also, each flame had experienced more than one integral length scale (L = 20 mm [30]) and avoided interaction with the bomb fans to omit heat loss and flow field disturbance effects. Following an approach introduced in [31] an effective rms turbulent velocity, u'_k can be found by integrating the turbulent power spectrum density and subsequently used to characterise turbulent flame development (the observed continuous increase in burn rate from the point of ignition). For u'_k / u' = 1 the flame encompasses all magnitudes of turbulent eddies. As shown in Fig. 16, at r_{sch} = 30 mm, u'_k / u' was determined to be ~ 60% thus an appreciably proportion of the turbulent flow field had interacted with the flame. It could be shown that ranking fuels with respect to u_{te} at r_{sch} = 30mm is typical of their ranking at any other radii at 30 mm < r_{sch} < 65 mm [8].

The turbulent conditions of the flames explored in the presented work could be encapsulated with the aid of a Borghi Diagram [32]. The sample data of Fig. ? refer to conditions for the slowest and fastest fuels under laminar burning, 2.2 dimethyl butane and 1-hexyne, but are typical of the other fuels investigated. At u' = 2 m/s, most flames fell into the "Corrugated Flames" regime. At this condition, the laminar flame thickness $\delta_l < \eta$ (the Kolmogorov scale) and the Damköhler number $Da > 1$, signifying that the chemical and transport processes at the flame front should not be fundamentally disturbed, even by the smallest turbulence scales. At u' = 6 m/s most flames fall within the "Thickened Turbulent Flame" regime, with $\eta < \delta l$. Here the smallest turbulent length scales (Kolmogorov scale) may "penetrate" into the flame front, thus potentially altering the transport and chemical processes occurring within a thickening turbulent flame structure.

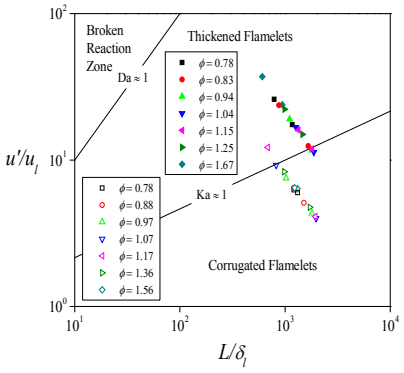

Fig. 6 – Turbulent combustion regime diagram for 2,2 dimethyl butane and 1-hexyne at u' = 2 m/s (unfilled symbols) and 6 m/s (filled symbols).

Displayed in Fig. 18 are the turbulent burning velocity results (u_{te}) for the C_6 dataset, at turbulent rms velocities of u' = 2 and 6 m/s, plotted versus ϕ. The curves are 3rd order polynomial fits to the experimental data. The experimental scatter in u_{te} (~10% in C.O.V.) proved independent of u' and in accord with turbulent cycle-to-cycle variations reported elsewhere [7]. As expected, turbulence significantly enhanced the burn rate of all fuels examined. The peak turbulent burning velocities at u' = 2 m/s were attained at 1.3 < ϕ < 1.4, around 0.2 in equivalence ratio richer compared to peak burn rates of laminar flames. As u' increased to 6 m/s, peak u_{te} values shifted further towards rich mixtures at 1.4 < ϕ < 1.5. This is a qualitative difference between turbulent and laminar flames. Overall, the increase in $u_{te,max}$ attained by increasing u' from 2 to 6 m/s accorded to $u_{te,max} \sim (u')^{0.72}$, similar to that described in [33].

This displacement of the maximum burning rate towards rich mixtures was observed as early as 1955 [34]. However, until relatively recently [35], this observation received little attention. One possible explanation is based on the assumption that the turbulent burning rate is governed by the critically curved "leading points" of the flame front, i.e. those parts of the flame most advanced into the fresh gas [36]. Subsequently, an alternative suggestion was made that the leading points are critically curved rather than strained [32]. Both hypotheses predict that for HCs with molar mass heavier than that of O_2, the peak turbulent burning rates should be exhibited by rich flames.

Comparison between the laminar and turbulent burn rate results showed that the fuel breakdown mechanism remains significant even for turbulent flames. Ranking between fuels remained largely unaffected with the highly unsaturated fuels distinctively remaining the fastest and the branched HCs clearly remaining the slowest. At lean turbulent conditions, differences between the burn rates of the fuels remained similar to

those observed under lean laminar conditions. However, at rich turbulent conditions, differences in u_{te} were notably smaller than differences in u_l. Indicatively, at $\phi = 0.78$, 1-hexyne was faster by 50%, 60% and 75% c.f. 2,2 dimethyl butane at laminar, $u' = 2$ m/s and $u' = 6$ m/s conditions, respectively. The respective differences in burn rate at $\phi \approx 1.4$, where 80%, 20% and 20%. Quantification of the burn rate gain under turbulence is presented with the aid of u_{te} / u_l data (Fig. 8). At $u' = 6$ m/s, for $\phi < 1.0$, average ratios of u_{te} / u_l between the C_6 fuels were within 15%, while for the richer conditions explored ($\phi = 1.67$) differences in u_{te} / u_l up to 90%. A more generalised way of showing the propensity of rich flames to gain more under turbulence is presented in Fig. ?, which includes data of u_{te} / u_l vs. u'_k / u_l for all fuels examined. Lean flames clearly show no increase in u_{te} / u_l with u'_k / u_l; the opposite is true for rich flames, where an almost linear increase in burn rate gain under turbulence was observed.

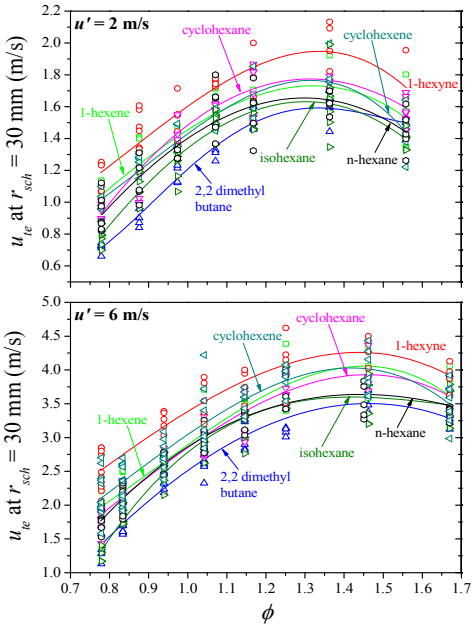

Fig. 7 – Turbulent burning velocities of the C_6 fuels at mean flame radii of 30 mm, plotted against ϕ.

Exemplar contours of successive flame edges generated from schlieren images of n-hexane flames are shown in Fig. ??. Lean flames at $\phi = 0.78$ (Le > 1), exhibited intense local protrusions and recesses with signs of local extinction. This is in distinct contrast to the development of rich flames at $\phi = 1.36$ (Le < 1) which exhibited clear and well defined flame contours. In such cases, the degree of burn rate enhancement due to turbulence proved much higher. Therefore, although the conditions at $\phi = 0.78$ and $\phi = 1.36$ fall at almost the same location in the turbulent regime diagram, the nature of flame propagation appeared to be rather different between these two cases. Similar observations were recently made by Law et al [6], suggesting that the effects of non-equidiffusion should be incorporated in a more generalised form of the regime diagram.

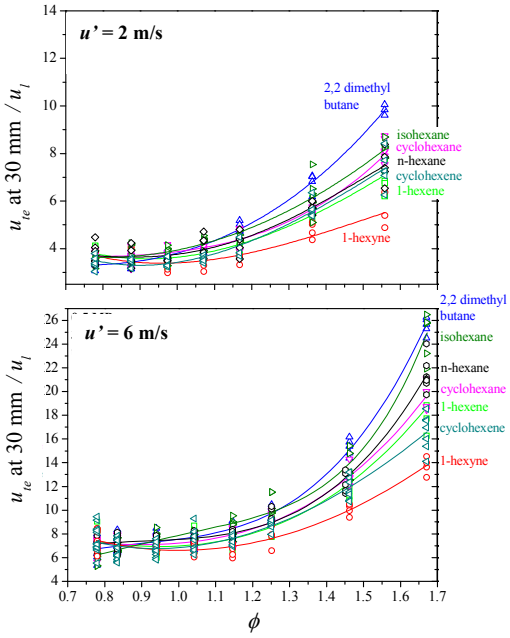

Fig. 8 – Ratio of turbulent to laminar burning velocities plotted against ϕ.

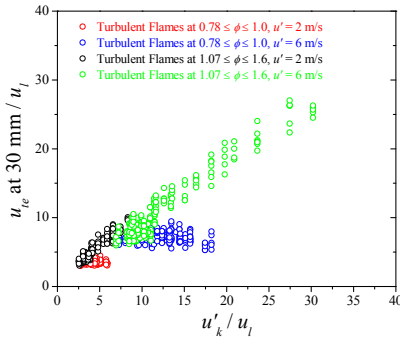

Fig. 9 – Overall correlation of u_{te} / u_l with u'_k / u_l for the C_6 hydrocarbons.

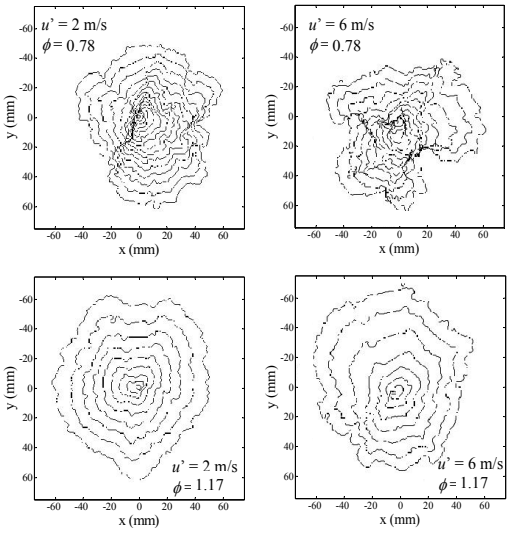

Fig. 10 – Sample flame contours of n-hexane turbulent flames. Flame morphology at each condition was typical to that observed for all C_6 fuels.

Conclusions

Molecular structure was shown to significantly affect the laminar burn rate of C_6 HC fuels. Laminar burning velocity loosely correlates with T_{ad}, however chemical kinetic effects are also of high importance, in certain cases being the dominant factor. It was found that the degree of unsaturation of a fuel (triple or double bond or ring structure) enhances laminar burn rate, while branched (isomeric) structure inhibits it. Under laminar conditions at 0.5 MPa, cellularity enhances the burn rate. Findings from the current study suggest that for the rig used in this study, the fuels and conditions explored, cellularity-induced flame acceleration lasted for around 10-15 mm in flame radius following the cellularity onset, before returning back to values similar to those observed during the pre-cellular phase.

The turbulent flames examined fell into the corrugated or thickened flamelets regime categories, where flame structure is generally assumed to be unaffected. It was found that turbulence significantly enhanced the burn rate. Increasing turbulence increased the turbulent burning velocity to an extent described by $ute \sim (u')^{0.72}$. Also, turbulence shifted the peak burn rates of all fuels examined to richer mixtures compared to peak burn rates of laminar flames. This shift accounted to ca. 0.2 and 0.3 in equivalence ratio for u' = 2 m/s and 6 m/s, respectively. Lean turbulent flames generally showed similar relative differences between the fuels independently of the flow field conditions. On the other hand, for rich fuel-air mixtures, the relative differences between the fuels were found to decrease going from laminar to turbulent as well as with increasing turbulent rms velocity. Nonetheless, the C_6 fuels were observed to overall retain their laminar ranking at a given equivalence ratio even at the highest turbulent velocity explored, suggesting influence of the molecular structure under turbulent burning.

Acknowledgements

The support of EPSRC and Mercedes-Benz High Performance Engines is gratefully acknowledged.

References

[1] M. Gerstein, O. Levine, E.L. Wong, J Am Chem Soc 73 (1951) 418

[2] S.G. Davis, C.K. Law, Combust Sci Tech 140 (1998) 427

[3] C.M. Vagelopoulos, F.N. Egolfopoulos, P Combust Inst 27 (1998) 513

[4] J.T. Farrell, R.J. Johnston, I.P. Androulakis, SAE Tech Paper (2004) 2004-01-2936

[5] F. Wu, A.P. Kelley, C.K. Law, Combust Flame 159 (2012) 1417

[6] F. Wu, A. Saha, S. Chaudhuri, C.K. Law, P Combust Inst 35 (2015) 1501

[7] M. Lawes, M.P. Ormsby, C.G.W. Sheppard, R. Woolley, Combust Sci Technol 177 (2005) 1273

[8] C. Mandilas, PhD Thesis, University of Leeds, "Laminar and Turbulent Burning Characteristics of Hydrocarbon Fuels", 2008

[9] D. Bradley, P.H. Gaskel, X.J. Gu, Combust Flame 104 (1996) 176

[10] D. Bradley, R.A. Hicks, M. Lawes, C.G.W. Sheppard, R. Woolley, Combust Flame 115 (1998) 126

[11] C. Mandilas, M.P. Ormsby, C.G.W. Sheppard, R. Woolley, Proc Comb Inst 31 (2007) 1443

[12] T. Kitagawa, T. Nakahara, K. Maruyana, K. Kado, A. Hayakawa, S. Kobyashi, Int J Hydrogen Energ 33 (2008) 5842

[13] S. Jerzembeck, N. Peters, SAE Technical Paper (2008) 2008-01-0471

[14] Z. Chen, L. Wei, Z. Huang, H. Miao, X. Wang, D. Jiang, Energ Fuel 23 (2009) 735

[15] E. Varea, V. Modica, A. Vandel, B. Renou, Combust Flame 159 (2012) 577

[16] A Moghaddas, K. Eisazadeh-Far, H. Metghalchi, Combust Flame 159 (2012) 1437

[17] A.P. Kelley, A.J. Smallbone, D.L. Zhu, C.K. Law, P Combust Inst 33 (2011) 963

[18] D. Bradley, C.G.W. Sheppard, R. Woolley, D.A. Greenhalgh, R.D. Lockett, Combust Flame 122 (2000) 195

[19] S. Coronel, N. Bitter, V. Thomas, R. Mevel, J.E. Shepherd, Paper #087LF0020, WSSCI Meeting, 2014

[20] Bird, R.B., Stewart, W.E., Lightfoot, E.N., Transport Phenomena, 2nd Ed., Wiley & Sons, 2002

[21] C.K. Law, 22nd Symp (Inter) Comb, The Combustion Institute, 1381-1402, 1988

[22] D. Bradley, C.M. Harper, Combust Flame, 99 (1994) 562

[23] F.L. Dryer, C.K. Westbrook, Prog Energ Combust 10 (1984) 1

[24] R.J. Johnston, J.T. Farrell, P Combust Inst 30 (2005) 217

[25] E. Hu, Z. Huang, J. He, H. Miao, Int J Hydrogen Energ 34 (2009) 8741

[26] A.A. Burluka, A.M.T.E. Hussin, C.G.W. Sheppard, K. Liu, V. Sanderson, Flow Turb Combust 86 (2011) 735

[27] M. Fairweather, M.P. Ormsby, C.G.W., Sheppard, R. Woolley, Combust Flame 156 (2009) 780

[28] A.N. Lipatnikov J. Chomiak Combust Sci Technol 137 (1998) 277

[29] N. Lamourex, N. Djebaili-Chaumeix, C.E. Paillard, Exp Therm Fluid Sci 27 (2003) 385

[30] K. Nwagwe, H.G. Weller, G.R. Tabor, A.D. Gosman, M. Lawes, C.G.W. Sheppard, R. Woolley, P Combust Inst 28 (2000) 59

[31] R.G. Abdel-Gayed, D. Bradley, M. Lawes, Proc R Soc Lond A414 (1987) 389

[32] R. Borghi, Prog Energ Combust 14 (1988) 245

[33] V.L. Zimont, Exper. Therm Fluid Sci 21 (2000) 179

[34] K. Wohl, L. Shore, Ind. Eng. Chem. (1955) 828

[35] A.N. Lipatnikov, J. Chomiak, Prog Energ Combust 31 (2005) 1

[36] K.N. Bray, N. Peters, Turbulent Reactive Flows – Laminar Flamelets in Turbulent Flows, Academic Press, 1994